

Label-Efficient Point Cloud Semantic Segmentation: An Active Learning Approach

Xian Shi¹, Xun Xu², Ke Chen¹, Lile Cai², Chuan Sheng Foo², Kui Jia¹

¹South China University of Technology

²National University of Singapore

ausxian@mail.scut.edu.cn, alex.xun.xu@gmail.com, chenk@scut.edu.cn,
{caill, foo_chuan_sheng}@i2r.a-star.edu.sg, kuijia@scut.edu.cn

Abstract

Semantic segmentation of 3D point clouds relies on training deep models with a large amount of labeled data. However, labeling 3D point clouds is expensive, thus smart approach towards data annotation, a.k.a. active learning is essential to label-efficient point cloud segmentation. In this work, we first propose a more realistic annotation counting scheme so that a fair benchmark is possible. To better exploit labeling budget, we adopt a super-point based active learning strategy where we make use of manifold defined on the point cloud geometry. We further propose active learning strategy to encourage shape level diversity and local spatial consistency constraint. Experiments on two benchmark datasets demonstrate the efficacy of our proposed active learning strategy for label-efficient semantic segmentation of point clouds. Notably, we achieve significant improvement at all levels of annotation budgets and outperform the state-of-the-art methods under the same level of annotation cost.

1. Introduction

3D point cloud has been intensively investigated recently due to its application in autonomous driving, robotics, etc. The prevailing methods target point cloud learning tasks as designing backbone networks [3, 23, 22] which requires a large amount of labelled data for training. Although unsupervised contrastive feature learning [26] has drawn attention from the community, it still requires labeled data to train linear classifier. More importantly, labeling 3D point cloud, in particular for segmentation tasks, is inherently challenging as localizing data points in 3D space is inconvenient and prone to mistakes. Inspired by the annotation bottleneck, an initial attempt to use partially labeled dataset for semantic segmentation was made by [10]. A recent work [27] further revealed that it is not necessary to have access to

the label of all data points and proposed to combine several existing techniques to exploit the limited labeled points and a large number of unlabelled points for point cloud semantic segmentation. Another line of works evaluated a pre-train with finetuning strategy, where a large amount of unlabeled data is used to pre-train in an unsupervised manner and only a fraction of labelled data used for finetuning [30, 18, 26], thus achieved the purpose of saving annotation cost. Alternative to the assumption of partially labelled point cloud, weakly/inexactly label at sub-cloud level was exploited to reduce the annotation cost [24].

Among recent attempts to utilize fewer labelling effort, we figure out that there is no consensus on how to fairly count the cost of data annotation. From the semi-supervised learning point of view, annotation cost is often counted as the percentage of labelled shapes [10, 30, 26]. The underlying assumption is that the cost for labelling segmentation mask for each individual shape is equivalent. While the weakly supervised approach [27] assume the labelling cost as the number points annotated with ground-truth. We believe either assumption is not realistic enough to fairly benchmark various methods aiming to use less labeled data. As a result, in this work, we are inspired by recent study in active learning for image segmentation [4] and propose to count the annotation cost as the number of mouse clicks. For example, a 3D shape with either partial or full accurate segmentation mask, the annotation cost is counted as the number of labeled points if no special specification is mentioned.

Given the more realistic definition of annotation cost, the challenge is how to selectively annotate data to maximize the performance, a.k.a. active learning. It has been extensively studied as a generic problem [19, 7] and some efforts were dedicated to segmentation in 2D image domain [28, 12, 21]. However, to the best of our knowledge, active learning for 3D point cloud is overlooked by the community, which is the focus of this work. More importantly, to

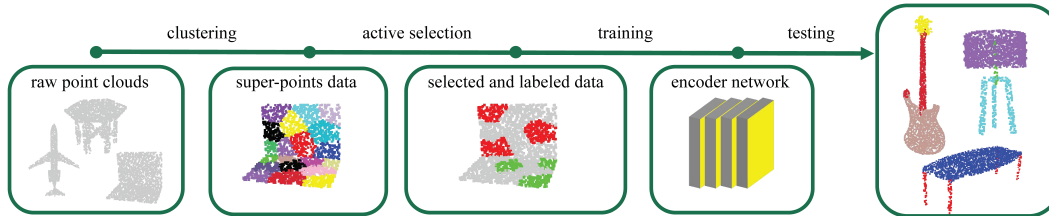


Figure 1. The overview of active learning for 3D point cloud segmentation.

best exploit the annotation budget, directly making clicks on individual point is no longer the optimal solution. Instead, we believe both the geometric nature and label smoothness are important clues to data annotation. Therefore, we propose to provide annotations at the level of super-point. Each super-point consists of a group of points and represents a geometric homogeneous region on the shape. Thus the super-point is very likely to have the same semantic label and annotation at such coarse level, i.e. assigning a single label to one super-point, could better exploit the limited budget. To further improve the efficacy of active learning algorithm in selecting diverse data samples, we introduce additional shape diversity terms to complement the widely adopted feature diversity and uncertainty measurements. Finally, we are also inspired by the success of smoothness constraint in [27] and propose a consistency constraint within a super-point to enforce semantic predictions within a super-point to agree. Both are proved to be effective for active learning on 3D point cloud segmentation. In summary, we make the following contributions:

- To the best of our knowledge, this is the first attempt to consider annotation cost for 3D point cloud segmentation in a realistic way compared to existing works. Our final model outperforms all existing methods under the proposed cost counting scheme.
- We introduce an active learning framework to best exploit the annotation budget. Importantly, super-point based labeling is adopted to substantially save annotation budget.
- Consistent predictions within each super-point is enforced to further exploit the geometric homogeneity and consistently improve active learning performance.

2. Related Work

2.1. Active Learning

Active learning has been extensively studied to optimally exploit the annotation budget. It aims to select the most informative data samples from all unlabeled data for an oracle to annotate. Commonly adopted active learning approaches consider diversity [2] and uncertainty [9] as the clue to guide the selection. In specific, [19] proposed to

maximize the diversity of selected samples in feature space and formulated the problem as a K-center problem. Uncertainty is often measured by the entropy of classifier’s posterior. A recent work adopted an adversarial training strategy to measure the uncertainty where samples that can be easily attacked should be labelled [6]. In this work, we discover that the spatial adjacency property on point cloud is not considered in generic active learning research. Therefore, we propose to use the spatial property as additional property to guide the active selection.

2.2. 3D Point Cloud

3D point cloud can be collected from LiDAR sensor and has been applied in autonomous driving, robotics, etc. Deep learning on 3D point cloud is mostly focused on developing backbone networks, e.g. PointNet [15], PointNet++ [16], DGCNN [23], etc. These methods were demonstrated on recognition [25, 29], semantic segmentation [29, 13], object detection [14]. Among these semantic segmentation has wide applications in autonomous driving and robotics and it is particularly difficult to label segmentation masks in 3D point cloud. Therefore, we choose to demonstrate active learning on 3D point cloud semantic segmentation tasks.

Point Cloud Annotation Labeling 3D point cloud requires assigning labels to each individual point. For individual shape point clouds, [29] proposed an active framework to iteratively generate and validate manual and automatic annotation, achieving a point cloud annotation procedure with both efficiency and accuracy. For large scale scene point cloud, [1] first parsed the whole raw point clouds into individual physical spaces, and then annotated each independent space in the way of detection. However, there is no standard annotation method and no agreed metric to quantify the cost associated with 3D point cloud annotation.

Less Labelled Data Existing research often assume a large fully labelled dataset available which is sometimes too strong. It is known that labelling 3D point cloud is expensive and sometimes requires expertise [27]. As a result, the community recently turned to exploiting partially labelled data [27], inexactly labelled data [24] and weakly labelled data [17] for the sake of saving annotation cost. In addition,

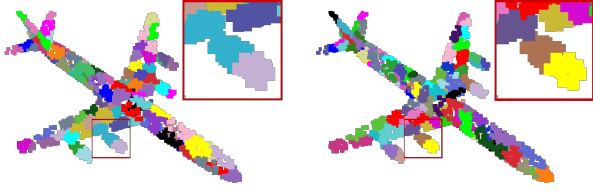


Figure 2. Super-points clustered with spatial coordinates v.s. with additional geometric features. Color indicates different super-points.

there are several ways to improve network performance with insufficient labeled data. Capsule network [11, 30] can maximally reserve valuable information and infer possible variables with less training data. [8] combines three unsupervised learning methods including clustering, reconstruction and self-supervised classification to improve network performance on less labelled data. Pre-training [26] is also proved to be able to deal with low capacity network when there are few labeled samples. Nevertheless, there is still no rigorous study of whether or how much annotation is saved by various annotation schemes. In this work, we provide a fair comparison of annotation cost and propose several ways to achieve better performance with less labeled data.

3. Methodology

In this section, we first describe how to generate Super-Points considering point cloud geometric information. Then we will elaborate active selection strategy based on super-points, which is achieved by optimizing feature diversity, uncertainty and shape diversity. Finally we illustrate how to utilize super-point consistency to further apply constraint for learning task.

3.1. Super-point Generation

Spectral Clustering We employ spectral clustering for super-point generation. Given a point cloud sample with N points $\mathcal{X}_i = \{\mathbf{p}_{ij}\}_{j=1\dots N}$, an affinity matrix \mathbf{A} is first computed characterizing the adjacency of data points. All points are then grouped into K non-overlapping clusters by normalized cut algorithm [20]. To construct the affinity matrix, one could build a k nearest neighbor graph based on the Euclidean distance defined over spatial coordinates and RGB values [27]. However, we argue that Euclidean distance alone is still prone to non-uniform point distribution and complex local geometric structures, thus making erroneous links. To remedy this issue, we propose to exploit the local geometric feature to take into account the local geometric structure.

Geometric Features To characterize the local shape of the region around a point, we compute three geometric features [5] by looking into the neighborhood. For a point

$\mathbf{p} = (x \ y \ z)$, we denote its k nearest neighbors as $\mathcal{N}\mathcal{N}_k(\mathbf{p})$. Given $\mathbf{M} = (\mathbf{p}_1 - \mathbf{p}, \dots, \mathbf{p}_n - \mathbf{p})^T$, where $\mathbf{p}_1 \dots \mathbf{p}_n \in \mathcal{N}\mathcal{N}_k(\mathbf{p})$, the covariance matrix is defined by $\mathbf{C} = \frac{1}{n}\mathbf{M}^T\mathbf{M}$. Since \mathbf{C} is a symmetric positive semi-definite matrix, its three eigenvalues exist and are non-negative. Without loss of generality, we define eigenvalues as $\lambda_1 \geq \lambda_2 \geq \lambda_3 \neq 0$. The linearity (f_1), planarity (f_2) and scatterness (f_3) derived from the eigenvalues are described as

$$f_1 = \frac{\lambda_1 - \lambda_2}{\lambda_1}, \quad f_2 = \frac{\lambda_2 - \lambda_3}{\lambda_1}, \quad f_3 = \frac{\lambda_3}{\lambda_1} \quad (1)$$

We define geometric feature vector as $\mathbf{g} = \{f_1, f_2, f_3\}$ which derives a geometric feature distance between individual points as $d_g(\mathbf{p}_i, \mathbf{p}_j) = \|\mathbf{g}_i - \mathbf{g}_j\|_2$ (2)

The final affinity matrix \mathbf{A} combines spatial distance and geometric feature distance as

$$a_{ij} = \exp\left(-\frac{\|\mathbf{p}_i - \mathbf{p}_j\|^2}{2\sigma_s^2}\right) + \gamma \exp\left(-\frac{\|\mathbf{g}_i - \mathbf{g}_j\|^2}{2\sigma_g^2}\right) \quad (3)$$

where σ_s and σ_g are bandwidth parameters. Each resultant cluster \mathcal{C} constitutes a super-point $\mathcal{S} = \{\mathbf{p}_i\}_{i \in \mathcal{C}}$. An example comparing super-points generated with spatial coordinate alone and with additional geometric features are shown in Fig. 2. Obviously, the latter one produces boundary between ‘engine’ and ‘wing’ that better aligns with the ground-truth semantic boundary.

3.2. Active Selection

Active learning aims to select and label a fixed budget of data to train the model. In this section, we first present a more realistic annotation counting scheme. Then a novel active learning query function is derived from state-of-the-art diversity and uncertainty based criterion.

More Realistic Annotation Counting Scheme There is no consensus on a realistic scheme for counting the annotation cost. Shape-level semi-supervised learning methods [10, 26] assume the costs of all shapes are equal while point-level weakly-supervised method [27] assume all points contribute equally to annotation budget. Although active learning was employed to create ground-truth annotation for ShapeNet [29], there is no explicit discussion on cost counting and the brush painting approach may not generalize to more generic 3D point cloud data. Inspired by recent discussion in active learning for image segmentation [12, 4], we propose to count the number of mouse clicks as annotation budget. Under this more realistic scheme, the cost for shape-level annotation is calculated as the number of all labelled points, e.g. if M shapes each with N points are labeled, the cost is counted as $M \cdot N$. Since points in the same super-point have a high degree of consistency (as shown in Fig. 2), to more efficiently use the annotation budget, we

provide a single label to the whole super-point, thus one super-point only counts 1 click.

Active Learning for Shapes We first formally define the active point cloud annotation task. We denote all point cloud samples as $\mathcal{X} = \{\mathcal{X}_i\}$, e.g. airplane, car, etc. in ShapeNet dataset and cubicles in a room for S3DIS dataset, where $\mathcal{X}_i = \{\mathcal{S}_j\}$. Given limited labeling budget B , counted as the number of clicks in this context, we aim to select a subset of points, $\mathcal{X}_i^L \subset \mathcal{X}_i$, to annotate with \mathcal{Y}_i^L so that the performance on validation set is maximized. The annotation is usually provided in multiple batches and the active selection will repeat iteratively. The core of active learning research is on designing acquisition function to determine which data points to select for labeling. Both feature diversity [19] and uncertainty maximization [9] are widely adopted as the acquisition function with remarkable performance achieved on classification and image segmentation. Nevertheless, we found both strategies locate many selected points on a single shape, which is not conducive to the generalization ability of network. To address this issue, we propose a shape level diversity to balance the spread out of annotation over shapes. Eventually, we combine diversity, uncertainty, shape diversity as acquisition function for active learning.

Diversity emphasizes the scatter of distribution in sample space. [19] proposed to maximize diversity measure as the objective for active learning and approximated with a greedy algorithm which only depends on an unary diversity score. For a point \mathbf{p} , we denote $\varphi(\mathbf{p})$ as its high dimensional feature from network. Its diversity score is measured by L_2 distance as

$$D_{score}(\mathbf{p}) = \min_{\mathbf{p}_j \in \mathcal{X}_i} \|\varphi(\mathbf{p}) - \varphi(\mathbf{p}_j)\|_2 \quad (4)$$

To extend diversity score to super-points \mathcal{S} , we estimate a super-point feature by average pooling over all points it contains as

$$\varphi(\mathcal{S}) = \frac{1}{|\mathcal{S}|} \sum_{\mathbf{p} \in \mathcal{S}} \varphi(\mathbf{p}) \quad (5)$$

where $|\mathcal{S}|$ represents the number of points in super-point \mathcal{S} . Then for each super-point \mathcal{S} in unlabeled super-points pool \mathcal{X}_u , its diversity score is formulated as

$$D_{score}(\mathcal{S}) = \min_{\mathcal{S}_j \in \mathcal{X}_i} \|\varphi(\mathcal{S}) - \varphi(\mathcal{S}_j)\|_2 \quad (6)$$

Uncertainty Uncertainty measures network’s confidence for the samples. Denoting $f(\mathbf{p}) \in R^k$ as the posterior prediction for a point \mathbf{p} , where K is the number of predicted categories, it is common to adopt entropy as uncertainty score,

$$E(\mathbf{p}) = - \sum_{j \in k} f(\mathbf{p})^j \log(f(\mathbf{p})^j) \quad (7)$$

For super-points level, we measure a super-point uncertainty by average pooling its points level uncertainty as

$$E_{score}(\mathcal{S}) = \frac{1}{|\mathcal{S}|} \sum_{\mathbf{p} \in \mathcal{S}} E(\mathbf{p}) \quad (8)$$

Shape Diversity As shapes in the dataset are of varying degrees of complexity, active selection may focus more on the shapes that are harder to learn. To avoid too many queried points falling on one sample, we propose shape diversity score to estimate shape level diversity in labeled data. For a shape point cloud \mathcal{X} , we define its feature $\varphi(\mathcal{X})$ as maxpooling of all points in the shape, the same as a super-point feature. Then we define shapes that have at least one annotated point as labeled shapes \mathcal{Y}_l and the rest as unlabeled shapes \mathcal{Y}_u . The shape diversity score is measured in the same way as point diversity

$$S_{score}(\mathcal{X}) = \min_{\mathcal{X}_j \in \mathcal{X}_l} \|\varphi(\mathcal{X}) - \varphi(\mathcal{X}_j)\|_2 \quad (9)$$

It is worth mentioning that shape diversity score is a shape level value. All points in the same shape share one value.

Eventually, for each super-point, its score in active learning strategy is defined as

$$AL_{score} = (1 - \beta)D_{score} + \beta E_{score} + \delta S_{score} \quad (10)$$

where β and δ are hyper-parameters. Our active selection follows a greedy algorithm by iteratively selecting the super-point with highest score, as summarized in Algo. 1

Algorithm 1: Our Active Learning

Input: Super-points Data \mathcal{X} , Labels Budget B ,
Query Number n_{query} , Network
Hyper-parameters θ

Output: Labeled Points Set

Randomly initialize super-points as labeled data \mathcal{X}_L
and the rest as unlabeled pool \mathcal{X}_U

while $|\mathcal{X}_L| < B$ **do**

 # Train the network with current \mathcal{X}_L

$\hat{\theta} = \arg \min_{\theta} l(\mathcal{X}_L; \theta)$

 # Evaluate the super-points in \mathcal{X}_U and Compute
 the active scores \mathcal{S} by Eq. (10)

for $\mathcal{X}_i \in \mathcal{X}_U$ **do**

$Score_i = AL_{score}(\mathcal{X}_i)$

 # Query super-point with the highest score

$\mathcal{X}_{II} \leftarrow \text{argsort}(Score)$ & $|\mathcal{X}_{II}| = n_{query}$

 # Update data pool

$\mathcal{X}_L = \mathcal{X}_L \cup \mathcal{X}_{II}$ s.t. $\mathcal{X}_U = \mathcal{X}_U \setminus \mathcal{X}_{II}$

3.3. Geometric Consistency Constraint

As a large amount of data points are still unlabeled, we naturally consider taking advantage of semi and weakly su-

pervised methods to extract extra information from the inherent characters of point cloud. As we cluster super-points according to relative distances and local geometric shape in a point cloud, the points within a same super-point share high similarity, which inspires us to extend consistency loss on super-points. For a super-point \mathcal{S} covering N points, the posterior prediction is defined as $f(\mathcal{S}) \in R^{N \times C}$ where C is the number of semantic categories. To enforce point level predictions within a super-point to be close to each other, we consider constraining the rank of $f(\mathcal{S})$, which will reach the minimum if all predictions stay the same. Instead of directly minimizing the rank of $f(\mathcal{S})$, we minimize nuclear norm in Eq. (11), which is a convex approximate to matrix rank.

$$l_{nc} = \frac{1}{N} \text{tr}(\sqrt{f(\mathcal{S})^T f(\mathcal{S})}) \quad (11)$$

where tr is the trace of a matrix. Finally our network loss comprises cross entropy loss for segmentation and nuclear loss.

$$l_{total} = l_{seg} + \lambda_{nc} l_{nc} \quad (12)$$

4. Experiment

4.1. Dataset

We use two 3D point cloud datasets to validate the proposed active learning framework.

- **ShapeNet** [29] consists of 16881 CAD shape models (12137, 1870 and 2874 for training, validating and testing respectively) from 16 categories with 50 part categories. For each shape model, 2048 points are sampled from mesh.
- **S3DIS** [1] was proposed for indoor scene analysis. It contains 3D point cloud with xyz coordinate and rgb information from 6 areas covering 271 rooms. We take Area 5 as testing set while the rest as training set. As each room is divided into 1*1 meter blocks with 4096 points, we conduct super-points clustering and active learning at each block in our experiments.

4.2. Competing Methods

We first compare both single point based labeling scheme and several variants of super-point based schemes. In specific, we have the following methods to compete against.

1. **Vanilla Point Based Scheme** [27] assumes labeled points are uniformly selected from all data points. According to our labeling budget definition, each point counts a unit label cost. We also evaluate feature diversity (Core-Set) [19] and entropy [9] based active selection criterion.

2. **Shape Based Scheme** As a shape sample in ShapeNet contains 2048 points. For convenience, we count one labeled shape as 2000 label cost. And then we conduct active selection at shape level, where the diversity and uncertainty of a shape are respectively the average diversity and uncertainty of all the points it contains. Similarly, we count a unit block (contains 4096 points) in S3DIS as 4000 label cost and process in the same way as above.

3. **Super-point Based Scheme** On super-point data, we compare our active selection method with Random selection, feature diversity and entropy criterion. We further extend a data augmentation and our nuclear loss in the final results. Annotating one super-point with a single label counts a unit cost.

4.3. Configuration

Data Augmentation Data augmentation is a common way to avoid overfitting, especially when labels are insufficient. Although Gaussian perturbation is widely used in 2D images learning, it may not an appropriate augmentation for point cloud on the semantic segmentation task. When the semantic boundaries are distinct in point cloud space, Gaussian perturbation is likely to destroy them as points may shift in arbitrary directions. To deal with this issue, we define a 3×3 deviation matrix as

$$\mathbf{T} = \mathbf{I} + \mathbf{G} \quad (13)$$

where \mathbf{I} is a 3×3 identity matrix and \mathbf{G} is a Gaussian matrix of the corresponding size. Then a shape point cloud $\mathbf{X} \in R^{N \times 3}$ can be augmented by

$$\hat{\mathbf{X}} = \mathbf{X}\mathbf{T} \quad (14)$$

Through multiplying by the deviation matrix, a point cloud is transformed on rotation and scaling. As it is a linear transformation, the topology of the object is preserved, which holds the semantic boundaries. Besides, in consideration of the symmetry of most objects, we also apply the random mirroring on the corresponding axis.

Encoder Network In view of the high training efficiency and outstanding semantic segmentation performance of DGCNN [23], we choose it as our backbone network. For the efficiency of training, the network is trained 200 epochs on ShapeNet dataset and 100 epochs on S3DIS dataset.

Hyper-Parameters Before training, we offline compute the geometric features, where the Knn Graph and neighbors is constructed by $k = 10$. To balance the effects of geometric features in clustering, the hyper-parameter γ is set as 0.1. In our experiments, we cluster each shape from ShapeNet into 500 super-points and S3DIS into 1000 super-points. In training section, loss weight λ_{nc} is set as 1. During active selection, β and δ in the formula is respectively assigned as 0.25 and 1.

Evaluation Metric For all testing data, we calculate the mean categories Intersect over Union (mIoU) as the evaluation metric. It is counted as the average of all category IoUs among the data.

4.4. Active Learning for Semantic Segmentation

Part Segmentation Part segmentation attempts to assign part category label for the given 3D object. Each part category is considered as an independent class in the experiments. We evaluate active learning for part segmentation on ShapeNet with budgets as 10k/20k/50k/100k/200k respectively. As active learning iteratively picks samples for labeling, we randomly initialize the first labeled pool with 5k annotation budget, then in each iteration active learning selects candidate samples until the next budget set is reached. For example, with initialized 5k labeled data, network will be trained first. In the following selection phase, active learning will select another 5k samples to reach 10k budget. In the next iteration, additional 10k samples will be selected to reach the next 20k budget, until all budgets are exhausted. The results under different budgets compared with other competing approaches are presented in left of Tab.1.

Scenes Segmentation Our approach is also applicable to semantic segmentation in scenes. We conduct semantic segmentation experiments on S3DIS dataset. We set training data label budget as 50k/100k/200k/500k/1m respectively. The first labeled pool is randomly initialized with 25k budget and latter active selection pattern is the same as that in part segmentation mentioned above. The results are presented in right of Tab.1.

Analysis of Results Fully supervised baseline realizes the mIoUs of 82.3% and 49.1% respectively on ShapeNet dataset and S3DIS dataset. We make the following observations. 1) On ShapeNet data, our method on super-point data under 100k and 200k label budget achieved 79.9% mIoU which is higher than 95% relative performance of fully supervised approach (78.4%). On S3DIS data, the results also show the superiority of our method, achieving 47.5% mIoU with 1m label budget, ahead of 95% fully supervised performance(46.6%). 2) Super-point method is consistently better than point level and shape level active learning at all labelling budgets, thus suggesting directly labeling on super-point is more label efficient. 3) Our proposed AL algorithm is better than random, feature diversity and entropy criterion at all labelling budgets. This suggests the effectiveness of shape diversity for active selection. 4) When combined with consistency constraint (AL & Const), we achieve the best performance of all competing methods. It is also consistently better than AL alone on both datasets. 5) Shape level annotation scheme is much worse than the other two under our cost counting scheme. It probably due

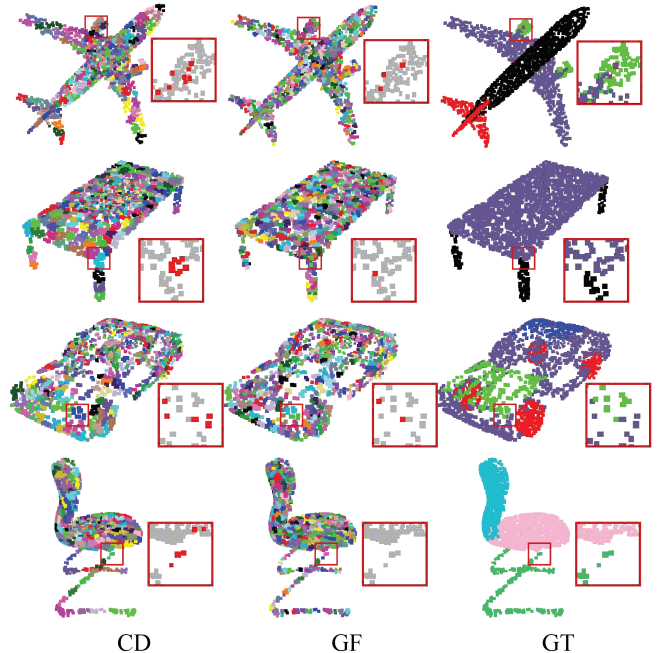


Figure 3. Super-points clustered with Coordinate(CD) v.s. with Geometric Features(GF) v.s. Ground Truth(GT). Each shape is clustered into 500 super-points and different clusters are shown in different colors. The red points in magnifying boxes of the first and second columns represent the noise points caused by cross-boundary super-points.

to that annotation focused on limited number of shapes has negative impact on network learning.

4.5. Ablation Study

To analyze the contribution of each individual component, we conduct ablation experiments on ShapeNet part segmentation and present the results in Tab. 2. The initial result is the performance of 10k labeled points by random selection. We make the following observations. 1) Point level v.s. super-point (SP), we observe 1.1% improvement from point data to vanilla super-point data. 2) Adding geometric feature (Geo) further improves 4.6% mIoU compared with super-points generated with point coordinate alone. 3) When AL considers shape diversity (Our AL), it does better than random selection with 1.5% improvement. 4) Nuclear loss for super-point consistency (Const) and Data Augmentation (DA) respectively boosts 0.9% and 0.5% performance. And the combination of both achieves 1.3% improvement.

4.6. Additional Study

SOTA Learning with Less Labelled Data With limited annotation budget, some studies have explored point cloud under fewer labeled data. To make fair comparison with existing works, we convert our budget to percentage, i.e.

Table 1. Segmentation evaluation ($mIoU\%$) among different active learning strategies

Dataset		ShapeNet					S3DIS				
Full-Supervised		82.3					49.1				
95% of Full-Performance		$82.3 \times 0.95 \approx 78.2$					$49.1 \times 0.95 \approx 46.6$				
Annotations Budget		10k	20k	50k	100k	200k	50k	100k	200k	500k	1m
Point Level	Random	63.3	70.0	73.0	75.9	76.0	40.3	41.1	42.5	45.0	45.9
	Core-set	59.0	66.2	72.8	76.0	77.1	39.0	40.2	42.0	44.6	46.6
	Entropy	59.5	62.2	63.1	71.8	73.4	38.3	41.3	42.4	43.3	45.2
Shape Level	Random	32.4	33.1	43.9	45.8	59.5	13.6	19.6	22.2	25.9	31.2
	Core-set	27.7	33.4	34.5	37.1	44.7	14.0	19.7	20.5	22.8	28.9
	Entropy	31.0	32.0	38.0	44.1	47.5	13.7	15.2	17.0	23.6	24.3
Super-point	Random	69.0	70.8	74.8	76.1	77.0	41.5	43.4	44.3	45.6	46.4
	Core-set	65.2	67.3	70.1	76.3	77.4	39.0	40.6	43.2	44.5	45.3
	Entropy	65.6	68.4	74.3	75.7	77.8	40.1	41.5	43.7	44.7	45.2
	Our AL	70.5	71.3	76.4	77.1	79.4	42.5	43.8	44.6	45.9	47.2
	Our AL & Const	71.8	74.1	77.1	78.4	79.9	42.8	44.1	45.9	46.3	47.5

Table 2. Ablation Study with 10k annotations

SP	Geo	Our AL	Const	DA	mIoU(%)
-	-	-	-	-	63.3
✓	-	-	-	-	64.4
✓	✓	-	-	-	69.0
✓	✓	✓	-	-	70.5
✓	✓	✓	✓	-	71.4
✓	✓	✓	-	✓	71.0
✓	✓	✓	✓	✓	71.8

Table 3. Different weakly supervised methods comparisons with an at most 1% label budget.

Methods	mIoU (%)	budget
SO-Net [11]	64.0	1%
PointCapsNet [30]	67.0	1%
Multitask Unsupervised [8]	68.2	1%
PointConstrast(HC) [26]	74.0	1%
PointConstrast(PINCE) [26]	73.1	1%
PointWeaklySupervised [27]	74.4	0.8%
Ours	79.9	0.8%

we divide the number of clicks (number of labeled super-points) by the total number of points, so that all methods share the same denominator. ShapeNet training set consists of 12137 shapes and each shape contain 2048 points. So the total points (clicks) is 24856576 and our 200k budget setting is around 0.8% total budget. We compare our performances with SONet [11], 3DCNet [30] and PCWS [27] at 0.8% to 1% label budget of all training data. We present evaluation results and corresponding training label budgets at Tab.3. Our method performs best among all methods even with the least budget.

Comparisons of Different Super-points We examine the quality of super-points generated with and without geomet-

Table 4. Noise Points Rates (%) in different clusters. The first line is the number of super-points clustered in one shape.

Number of SP	50	100	200	500	1000
Coord	5.05	3.79	2.85	2.21	1.39
Geo	4.82	3.56	2.67	1.80	1.01

Table 5. Evaluation with 10k annotations among different numbers of super-points clustered in one shape.

Number of SP	50	100	200	500	1000
mIoU(%)	65.2	67.1	68.0	69.0	66.6

ric features by comparing the Noise Rate in the labeled data. As we annotate super-points with a single label, some points would be mislabeled, thus regarded as noise points in training data. For comparison, we cluster shape samples of training data into 50/100/200/500/1000 super-points and compare the noise rate with (w/Geo) and without (wo/Geo) geometric features with results reported in Tab.4. It is evident that at all granularity of super-point, geometric feature will improve the quality of super-point generation by reducing the noise rate.

Number of Super-Points We further evaluate effects of different numbers of super-points clustered in a shape. Given a fixed budget as 10k, we uniformly label super-points and train the network respectively. The evaluations between different super-point data are represented in Tab. 5. It is obvious that shapes clustered into 500 super-points achieves the closest to the optimal performance.

4.7. Qualitative Results

Visualize the generated super-points. We show super-point examples generated by different methods in Fig. 5. In the first column, super-points are clustered according to their spatial coordinate(CD) only. The second column

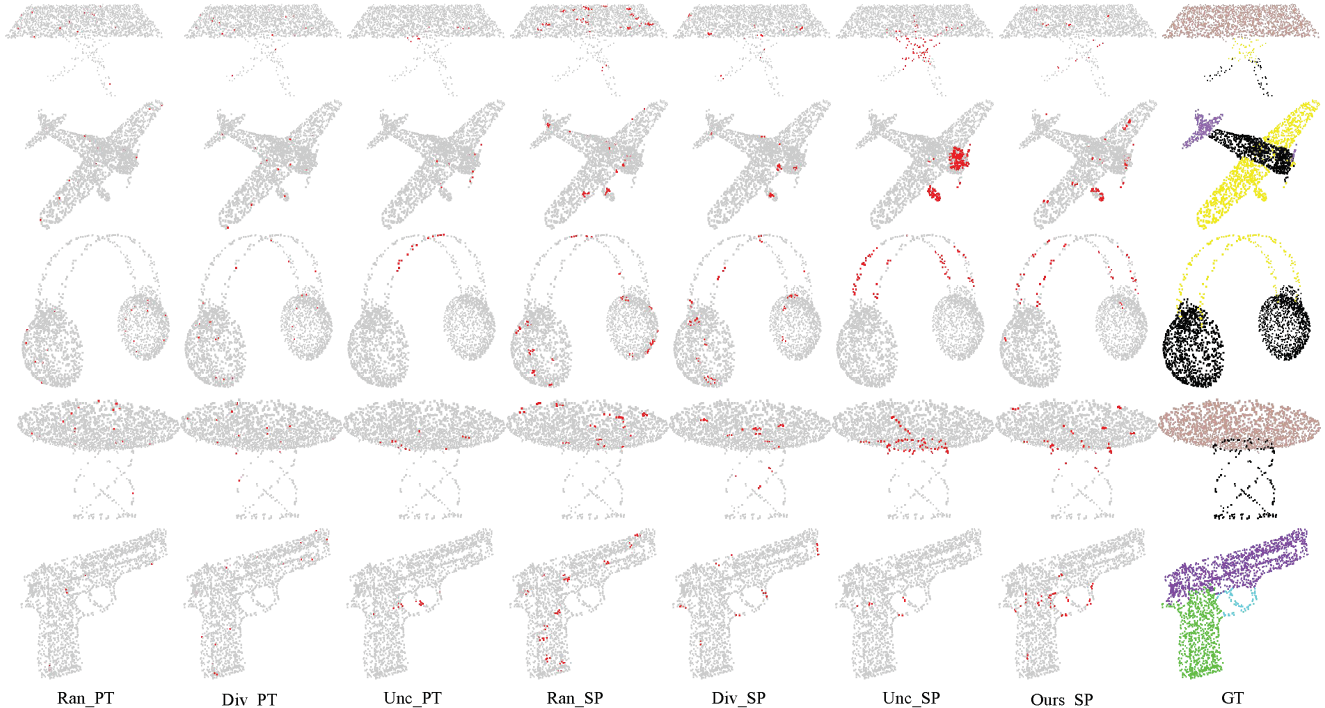


Figure 4. We visualize selected points/super-points under different active selection strategies in 200k label budget. Ran_PT, Div_PT and Unc_PT respectively represent random, diversity and uncertainty selection on point level data. And Ran_SP, Div_SP, Unc_SP and Ours_SP are the results of super-point level data selected with random, diversity, uncertainty and our method. The selected units are highlighted in red. In the final column objects semantic segmentation ground truth(GT) are shown.

presents the super-points generated with geometric features(GF). The final column is semantic ground truth (GT). In order to show the quality of the different super-points intuitively, we highlight the noise points caused by across boundaries super-points in red in the local enlarged views. It is observed that the number of points across categories can be effectively reduced by adding geometric features.

Visualize the selected points and super-points by different algorithms.

To show the distributions of points and super-points selected under different active learning strategies, we highlight the selected points and super-points on several objects in Fig.4, where the annotation budget is set as 200k. In the figure, the first to the third column from left to right respectively represent point level selection under random (Ran_PT), diversity (Div_PT) and uncertainty (Unc_PT) strategies. And the fourth to the seventh column is super-point level selection under random (Ran_SP), diversity (Div_SP), uncertainty (Unc_SP) and our method (Ours_SP). The selected points/super-points are marked in red. We also show object part semantic segmentation ground truth (GT) in the last column. It can be seen in the picture that randomly selected points/super-points tend to fall in dense areas. Diversity picks points/super-points that are scattered in the feature space, but it cannot distinguish whether these unit samples are difficult to learn for

the network. Uncertainty can find unpredictable samples but it is usually too concentrated in a small local region. Our method takes into account the advantages of both diversity and uncertainty, selecting super-points that are more conducive to learning.

5. Conclusion

In this work, we found that there is a lack of consensus on learning 3D point cloud segmentation with less labeled data thus making different methods less comparable. We proposed a more realistic annotation cost measurement by counting the number of clicks involved in producing the annotations. Under the new cost counting scheme, we proposed to provide labels at super-point level in an active learning fashion to best exploit the labeling budget. Geometric features are proved to help produce high quality super-points. We also introduce an unsupervised loss to encourage consistency of predictions within a super-point. Finally, we carried out experiments on two state-of-the-art 3D point cloud datasets and achieved more than 95% relative performance to fully supervised method with only 200k clicks, equivalent to 0.8% clicks one could make exhaustively. Our result also outperforms all existing works on point cloud segmentation with less labeled data.

References

- [1] Iro Armeni, Ozan Sener, Amir R Zamir, Helen Jiang, Ioannis Brilakis, Martin Fischer, and Silvio Savarese. 3d semantic parsing of large-scale indoor spaces. In *CVPR*, 2016. 2, 5
- [2] Klaus Brinker. Incorporating diversity in active learning with support vector machines. In *Machine Learning, Twentieth International Conference*, 2003. 2
- [3] Christopher Choy, JunYoung Gwak, and Silvio Savarese. 4d spatio-temporal convnets: Minkowski convolutional neural networks. In *Proceedings of the IEEE Conference on Computer Vision and Pattern Recognition*, 2019. 1
- [4] Pascal Colling, Lutz Roese-Koerner, Hanno Gottschalk, and Matthias Rottmann. Metabox+: A new region based active learning method for semantic segmentation using priority maps. *arXiv preprint arXiv:2010.01884*. 1, 3
- [5] Jérôme Demantké, Clément Mallet, Nicolas David, and Bruno Vallet. Dimensionality based scale selection in 3d lidar point clouds. *ISPRS - International Archives of the Photogrammetry Remote Sensing and Spatial Information Sciences*, 2011. 3
- [6] Melanie Ducoffe and Frederic Precioso. Adversarial active learning for deep networks: a margin based approach. 2018. 2
- [7] Yarin Gal, Riashat Islam, and Zoubin Ghahramani. Deep bayesian active learning with image data. In *International Conference on Machine Learning*, 2017. 1
- [8] K. Hassani and M. Haley. Unsupervised multi-task feature learning on point clouds. In *2019 IEEE/CVF International Conference on Computer Vision (ICCV)*, 2019. 3, 7
- [9] Ajay J. Joshi, Fatih Porikli, and Nikolaos Papanikolopoulos. Multi-class active learning for image classification. In *IEEE Conference on Computer Vision and Pattern Recognition*, 2009. 2, 4, 5
- [10] Jiaxin Li, Ben M Chen, and Gim Hee Lee. So-net: Self-organizing network for point cloud analysis. In *Proceedings of the IEEE conference on computer vision and pattern recognition*, 2018. 1, 3
- [11] Ancheng Lin, Jun Li, and Zhenyuan Ma. On learning and learned representation by capsule networks. 2018. 3, 7
- [12] Radek Mackowiak, Philip Lenz, Omair Ghori, Ferran Diego, Oliver Lange, and Carsten Rother. Cereals-cost-effective region-based active learning for semantic segmentation. In *BMVC*, 2018. 1, 3
- [13] Kaichun Mo, Shilin Zhu, Angel X Chang, Li Yi, Subarna Tripathi, Leonidas J Guibas, and Hao Su. Partnet: A large-scale benchmark for fine-grained and hierarchical part-level 3d object understanding. In *CVPR*, 2019. 2
- [14] Charles R Qi, Or Litany, Kaiming He, and Leonidas J Guibas. Deep hough voting for 3d object detection in point clouds. In *Proceedings of the IEEE International Conference on Computer Vision*, 2019. 2
- [15] Charles R. Qi, Hao Su, Kaichun Mo, and Leonidas J. Guibas. PointNet: Deep learning on point sets for 3D classification and segmentation. In *CVPR*, 2017. 2
- [16] Charles Ruizhongtai Qi, Li Yi, Hao Su, and Leonidas J Guibas. Pointnet++: Deep hierarchical feature learning on point sets in a metric space. In *NIPS*, 2017. 2
- [17] Zengyi Qin, Jinglu Wang, and Yan Lu. Weakly supervised 3d object detection from point clouds. *arXiv preprint arXiv:2007.13970*, 2020. 2
- [18] Jonathan Sauder and Bjarne Sievers. Self-supervised deep learning on point clouds by reconstructing space. In *Advances in Neural Information Processing Systems*, 2019. 1
- [19] Ozan Sener and Silvio Savarese. Active learning for convolutional neural networks: A core-set approach. *arXiv preprint arXiv:1708.00489*, 2017. 1, 2, 4, 5
- [20] Jianbo SHI. Normalized cuts and image segmentation. *IEEE transactions on pattern analysis and machine intelligence*, 2000. 3
- [21] Yawar Siddiqui, Julien Valentin, and Matthias Nießner. Viewal: Active learning with viewpoint entropy for semantic segmentation. In *Proceedings of the IEEE/CVF Conference on Computer Vision and Pattern Recognition*, 2020. 1
- [22] Hugues Thomas, Charles R Qi, Jean-Emmanuel Deschaud, Beatriz Marcotegui, François Goulette, and Leonidas J Guibas. Kpconv: Flexible and deformable convolution for point clouds. In *Proceedings of the IEEE International Conference on Computer Vision*, 2019. 1
- [23] Yue Wang, Yongbin Sun, Ziwei Liu, Sanjay E Sarma, Michael M Bronstein, and Justin M Solomon. Dynamic graph cnn for learning on point clouds. *Acm Transactions On Graphics (tog)*, 2019. 1, 2, 5
- [24] Jiacheng Wei, Guosheng Lin, Kim-Hui Yap, Tzu-Yi Hung, and Lihua Xie. Multi-path region mining for weakly supervised 3d semantic segmentation on point clouds. In *Proceedings of the IEEE/CVF Conference on Computer Vision and Pattern Recognition*, 2020. 1, 2
- [25] Zhirong Wu, Shuran Song, Aditya Khosla, Fisher Yu, Linguang Zhang, Xiaoou Tang, and Jianxiong Xiao. 3d shapenets: A deep representation for volumetric shapes. In *Proceedings of the IEEE conference on computer vision and pattern recognition*, 2015. 2
- [26] Saining Xie, Jiatao Gu, Demi Guo, Charles R Qi, Leonidas J Guibas, and Or Litany. Pointcontrast: Unsupervised pre-training for 3d point cloud understanding. *arXiv preprint arXiv:2007.10985*, 2020. 1, 3, 7
- [27] Xun Xu and Gim Hee Lee. Weakly supervised semantic point cloud segmentation: Towards 10x fewer labels. In *Proceedings of the IEEE/CVF Conference on Computer Vision and Pattern Recognition*, 2020. 1, 2, 3, 5, 7
- [28] Lin Yang, Yizhe Zhang, Jianxu Chen, Siyuan Zhang, and Danny Z Chen. Suggestive annotation: A deep active learning framework for biomedical image segmentation. In *International conference on medical image computing and computer-assisted intervention*, 2017. 1
- [29] Li Yi, Vladimir G Kim, Duygu Ceylan, I Shen, Mengyan Yan, Hao Su, Cewu Lu, Qixing Huang, Alla Sheffer, Leonidas Guibas, et al. A scalable active framework for region annotation in 3d shape collections. *ACM Transactions on Graphics*, 2016. 2, 3, 5
- [30] Yongheng Zhao, Tolga Birdal, Haowen Deng, and Federico Tombari. 3d point capsule networks. In *Proceedings of the IEEE conference on computer vision and pattern recognition*, 2019. 1, 3, 7

Appendix

A. Additional Qualitative Results for Super-Point

We show more examples, on ShapeNet, clustered with spatial coordinate only (CD) v.s. with additional Geometric features(GF) and the corresponding semantic ground truth(GT) in Fig. 5. For each shape in training set, We cluster it into 500 super-points without overlap. Since we assign each super-point with the majority label of the points it contains, those super-points that span across semantic boundaries lead to a small number of wrongly labeled points, which are marked in red in the figure. It can be seen from the figure that the super-points generated by geometric features better resembles the semantic boundaries, resulting in fewer red points.

B. Additional Qualitative Results for Active Learning

We present more qualitative active selection results for ShapeNet and S3DIS in Fig. 6 and Fig. 7. We fix total annotation budget for ShapeNet and S3DIS data respectively at 200K and 1m. Good active learning algorithms are expected to select a diverse while informative set of points/super-points.

In Fig. 6, the 1st to the 6th columns show the points/super-points selected by random (Ran_PT/Ran_SP), diversity (Div_PT/Div_SP) and Uncertainty (Unc_PT/Unc_SP) strategies on ShapeNet. The 7th column displays our method conducted on super-points(Ours_SP) and the last column is ground-truth (GT). The selected points/super-points are marked in red. It can be seen from the picture that, compared with individual points, super-points have a strong covering ability. A small number of labeled super-points can cover a substantial surface of the object, which is conducive to the efficient learning of a network. In the meantime, we can find that Diversity strategy (Div_PT/Div_SP) tends to select the points/super-points of scattered distribution, but ignores the complex areas of the object. Uncertainty (Unc_PT/Unc_SP) can find more ambiguous areas (such as aircraft wheel) in the object, but it is more likely to spend a large amount of annotation budget in one position, resulting in the lack of diversity of selected points. Our method takes into account the advantages of both methods and combines shape diversity to select a set of super-points with high complexity and diversity.

We also visualize the super-points selected for S3DIS dataset. Since we divide the S3DIS data into cubicles during training, for visualization in the whole room we stitch cubicles together to recover the labeled super-points in each room. Selected super-points under different strategies are

visualized in Fig. 7. It demonstrates that under random selection, the selected points are more likely to fall on the structure covering larger area such as ceiling and floor due to the imbalanced distribution of semantic classes. In contrast, our method does better in selecting more super-points to label from minority categories, e.g. the whiteboard in the 1st column of Fig. 7.

C. Qualitative Results for Segmentation

We present qualitative segmentation results with model trained on selected points/super-points on ShapeNet and S3DIS in Fig. 8 and Fig. 9. For ShapeNet, we fix the labeling budget at 200k and present the methods with best performance at different levels. At point level the best active selection strategy is diversity (Diversity Point). Random selection performs best at shape level data (Random Shape). Our method does the best at super-point level (Ours Super-point). We also show the Fully Supervision results and Ground-Truth in Fig. 8. It can be observed that our method outperforms all alternative active learning methods, and the segmentation results are closer to that of fully supervised results. The segmentation results in details of the ‘gun’ are even better than the results of full supervision.

For S3DIS, under 1m label budget, we present the best segmentation performance at point (Diversity Point), shape (Random Shape) and super-point (Ours Super-point) levels, as well. The segmentation ground-truth and real-scan RGB images are shown in the last two columns. It can be clearly seen in the figure that our method has obvious advantages over other methods in ‘window’ and ‘table’. These results demonstrate the superiority of our methods in semantic segmentation task.

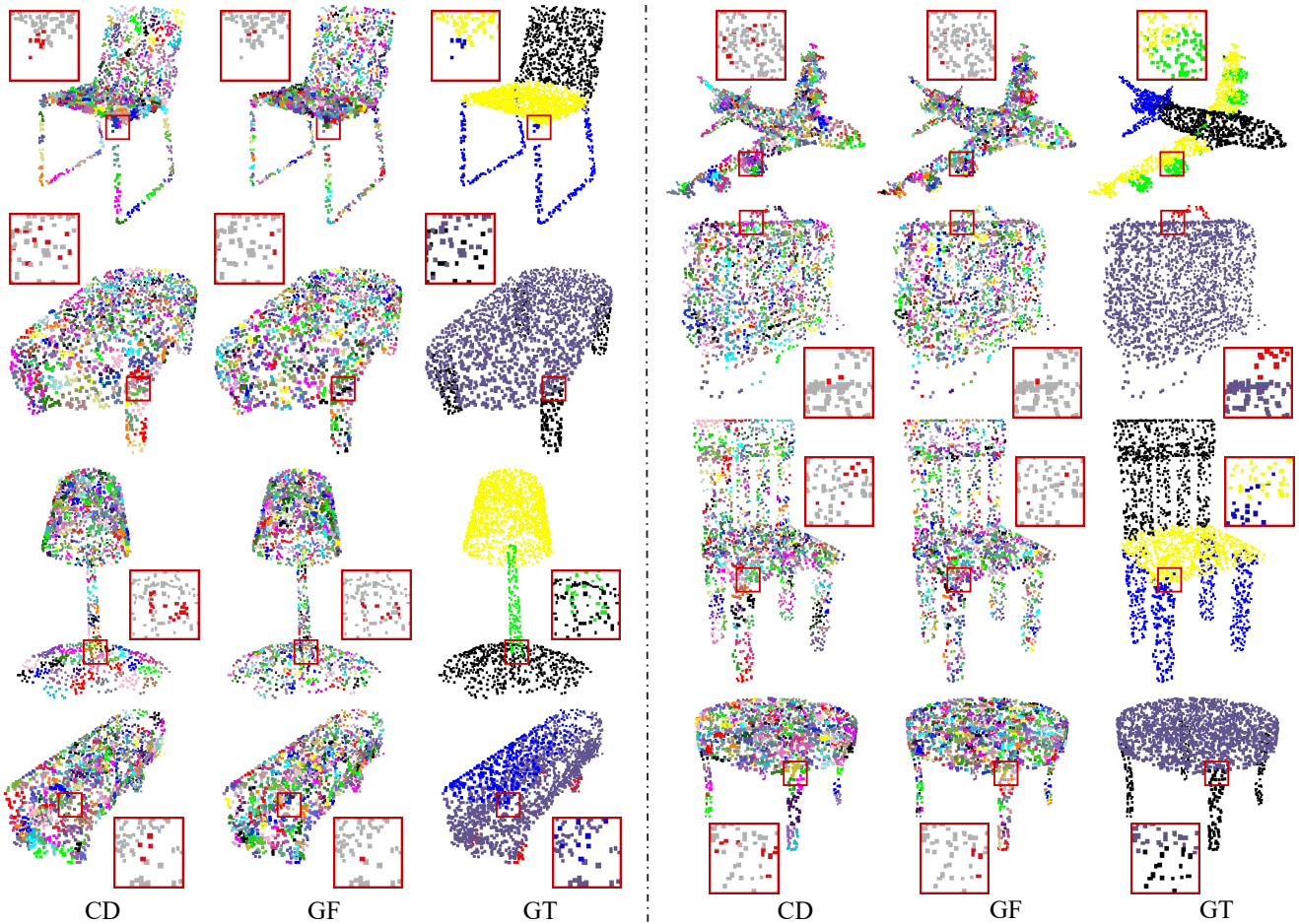


Figure 5. Super-points clustered with spatial coordinate (CD) v.s. with Geometric Features (GF) v.s. Ground Truth (GT). Each shape is clustered into 500 super-points and different clusters are shown in different colors. The red points in zoomed-in boxes of the first and second columns represent the wrongly assigned points caused by super-points spanning across semantic boundary.

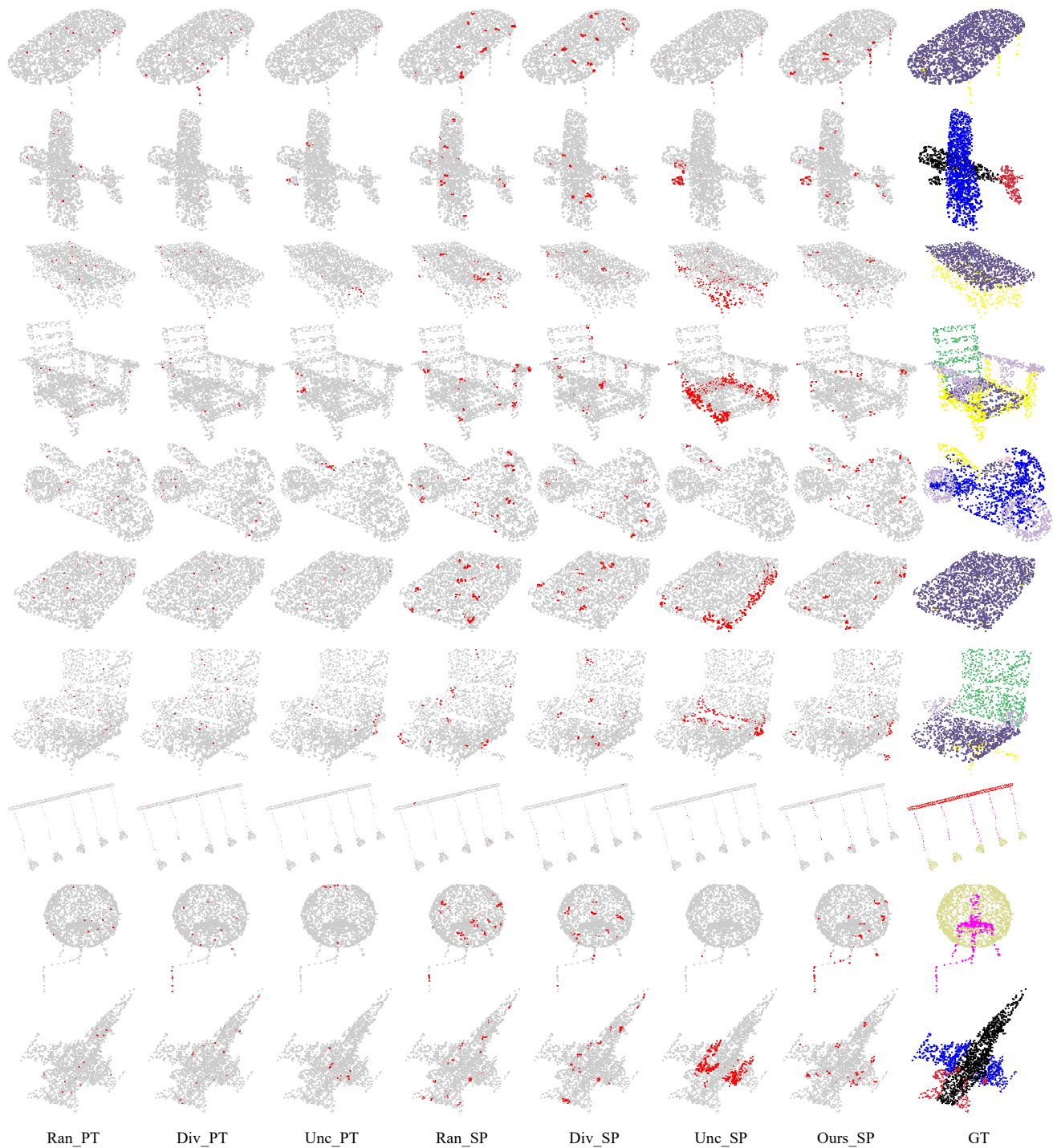


Figure 6. We visualize selected points/super-points under different active selection strategies in $200k$ labeling budget on ShapeNet data. Ran_PT, Div_PT and Unc_PT respectively represent random, diversity and uncertainty selection on point level data. And Ran_SP, Div_SP, Unc_SP and Ours_SP are the results of super-point level data selected with random, diversity, uncertainty and our method. The selected units are highlighted in red. In the final column objects semantic segmentation ground truth (GT) are shown.

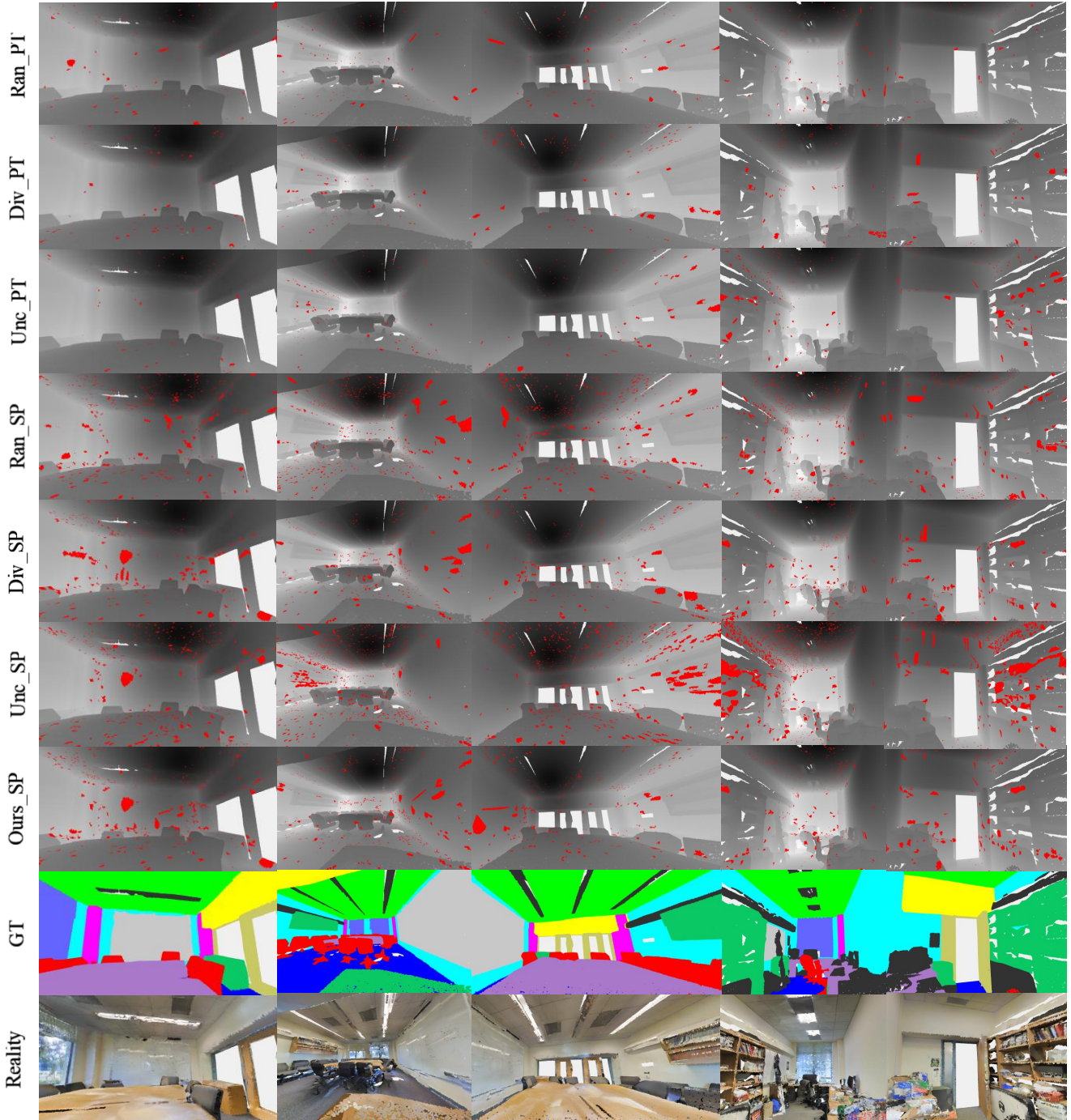


Figure 7. We visualize selected points/super-points under different active selection strategies with $1m$ labeling budget on S3DIS data. Ran_PT, Div_PT and Unc_PT respectively represent random, diversity and uncertainty selection on point level data. And Ran_SP, Div_SP, Unc.SP and Ours.SP are the results of super-point level data selected with random, diversity, uncertainty and our method. The selected units are highlighted in red. The last two lines show the semantic ground truth (GT) and the real scan RGB images.

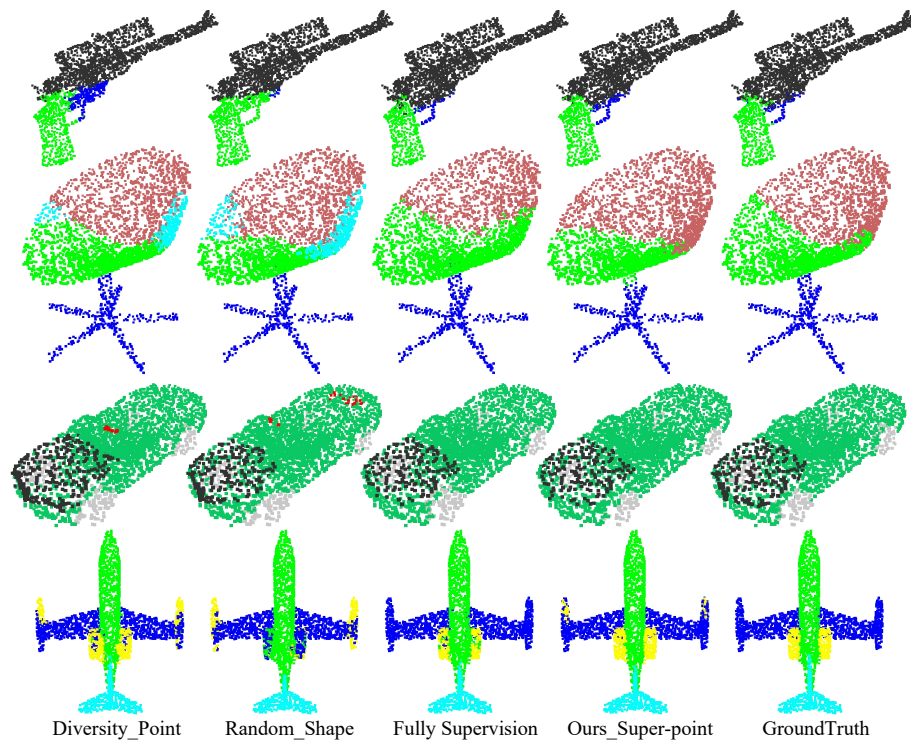


Figure 8. We present part segmentation results on ShapeNet comparing different methods as Diversity Point(diversity selection on point level), Random Shape(random selection on shape level), Fully Supervision, Ours Super-point(our methods on super-point level) and Ground-Truth.

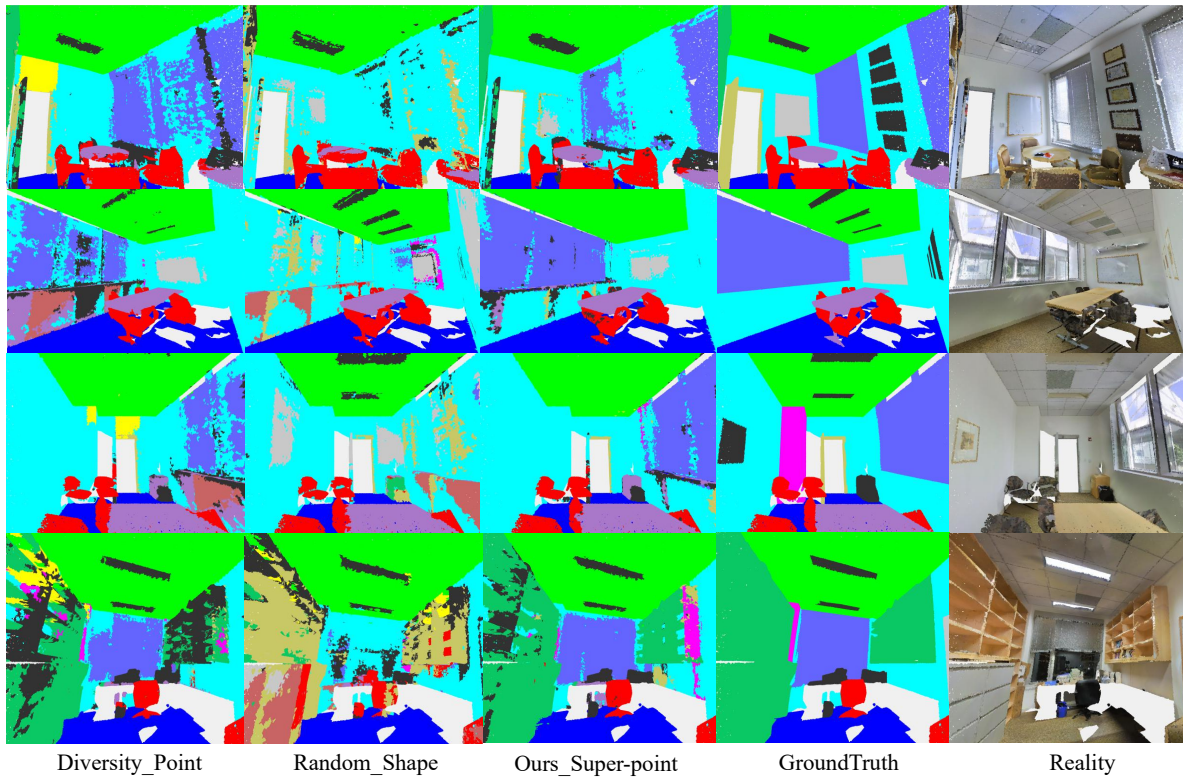


Figure 9. We present semantic segmentation results on S3DIS among different methods as Diversity_Point(diversity selection on point level), Random_Shape(random selection on shape level) and Ours_Super-point(our methods on super-point level). In the last two columns, segmentation ground-truth and real-scan RGB images are presented.